Pharmaceutical Research, Vol. 8, No. 3, 1991

Research Article

Calculation of the Aqueous Diffusion Layer Resistance for Absorption in a Tube: Application to Intestinal Membrane Permeability Determination

Jim H. Kou,[1] David Fleisher,[2] and Gordon L. Amidon[2]

Received June 14, 1990; accepted October 3, 1990

The single-pass intestinal perfusion technique has been used extensively to estimate the wall permeability in rats. The unbiased membrane parameters can be obtained only when the aqueous resistance is properly accounted for. This aqueous resistance was calculated numerically from a convective diffusive mass transfer model, including both passive and carrier-mediated transport at the intestinal wall. The aqueous diffusion layer resistance was shown to be best described by a function of the form,

$$\overline{P_{aq}^*}^{-1} = AG_z^{1/3} + BGz^C \left[P_c^* \left(\frac{K_m}{C_o}\right)^D + P_m^*\right]^E$$

where G_z, P_m^*, P_c^*, K_m, and C_o are, respectively, Graetz number, passive permeability, carrier-mediated permeability, Michaelis constant, and the drug concentration entering the tube. Asterisked are dimensionless quantities obtained by multiplying the permeability constants with R/D, where R and D being radius and drug diffusivity, respectively. A, B, C, D and E were obtained by a least-squares nonlinear regression method, giving values of 1.05, 1.74, 1.27, 0.0659, and 0.377, respectively, over the range of $0.001 \leq G_z \leq 0.5$, $0.01 \leq P_m^* \leq 10$, $0.01 \leq P_c^* \leq 10$, and $0.01 \leq K_m/C_o \leq 100$. This aqueous resistance was found to converge to those calculated from Levich's boundary layer solution in low Graetz range, indicating the correct theoretical limit. Using an iteration method, the equation was shown to be useful in extracting the intrinsic membrane permeability from the experimental data.

KEY WORDS: aqueous resistance; laminar tube flow; diffusion; intestinal absorption; carrier mediated transport; permeability; numerical method.

INTRODUCTION

The intestinal permeability of a compound is commonly estimated by a single-pass perfusion technique. Assuming that there is no radial convection due to water transport, the overall diffusional resistance to absorption can be visualized as a composite of two resistances in series, i.e.,

$$\frac{1}{P_{eff}} = \frac{1}{P_{aq}} + \frac{1}{P_w} \tag{1}$$

where P_{eff}, P_{aq}, and P_w denote effective, aqueous, and wall permeabilities, respectively. The effect of the aqueous resistance layer, also known as the unstirred or stagnant layer, has been clearly delineated both experimentally (1,2) and theoretically (3–6). P_{eff} can be calculated from experimental data according to a complete radial mixing model,

$$P_{eff} = -\frac{Q}{2\pi RL} \ell n \frac{C_m}{C_o} \tag{2}$$

where C_m/C_o is the measured fractional exit concentration, and Q, R, and L are flow rate, radius, and length, respectively (7). By separating out the aqueous contribution, the true wall permeability can be obtained. In the most general case, P_w is expressed by passive and carrier-mediated mechanisms in parallel, i.e.,

$$P_w = \frac{J_{max}}{K_m + C_w} + P_m \tag{3}$$

where J_{max}, K_m, and P_m are the maximum flux, Michaelis constant, and passive permeability, respectively. These quantities can be obtained by a nonlinear regression according to a variant form of Eq. (3) (9). If one ignores the aqueous layer, the membrane parameters obtained are biased, where K_m is always overestimated and P_m and J_{max} underestimated. Therefore, it is necessary to either eliminate or account for the effect of this aqueous resistance in order to arrive at the true membrane parameters.

Different approaches have been used to either minimize

[1] To whom correspondence should be addressed at Syntex Research, 3401 Hillview Ave., Palo Alto, California 94304.

[2] College of Pharmacy, The University of Michigan, Ann Arbor, Michigan 48109.

0724-8741/91/0300-0298$06.50/0

or account for the effect of this layer, such as maximizing the perfusion flow rate or simultaneous perfusion of fluid and air to introduce turbulence and reduce the concentration gradient in the lumen (1). Although these techniques have been shown to be effective in reducing the influence of the aqueous layer, the extent of this reduction is still unknown. Alternatively, one can account for the aqueous layer resistance theoretically through proper modeling of the hydrodynamics in the lumen. The advantage of the theoretical approach is that it allows unambiguous quantitation of the aqueous resistance, defined as $1/P_{aq}$, without resorting to an unknown "unstirred" layer thickness to fit the data.

Methods based on mass transport modeling to account for the aqueous resistance were previously developed (8,9). Based on the solution to a convective mass transfer problem with axial laminar flow in a straight tube, Elliott *et al.* (8) developed an approximate method for calculating the membrane permeability of passively absorbed compounds. The method is restricted to the passive diffusion at the intestinal wall because the solution scheme cannot accommodate nonlinear boundary conditions, such as one involved in Michaelis Menton absorption. Subsequently, Johnson and Amidon used the boundary layer approach similar to the one used by Levich (12) to solve a laminar tube flow problem including both passive and carrier-mediated components in the boundary condition (9). Upon linearizing the axial parabolic velocity profile, a solution was obtained analytically on semiinfinite coordinates. The aqueous resistance derived from the solution is expressed by

$$P_{aq}^{-1}(x) = 1.47 \frac{R}{D} G_z^{1/3} \left(\frac{x}{L}\right)^{1/3} \tag{4}$$

where R, L, D, and x are radius, length, aqueous diffusivity of the drug molecules, and axial coordinate, respectively; the Graetz number, G_z, is defined by

$$G_z = \frac{\pi DL}{2Q} \tag{5}$$

where Q is the volume flow rate in the tube. To improve the accuracy and extend the applicability of this method, the solution was adjusted by adding a parameter, A, to the aqueous resistance and matched to Elliott's solution in the first-order case. This results in the modified boundary layer solution (MBLS), and the aqueous resistance obtained is expressed as

$$P_{aq}^{-1} = A \frac{R}{D} G_z^{1/3} \tag{6}$$

with

$$A = 10.0G_z + 1.01, \quad 0.004 \leq G_z \leq 0.01$$
$$A = 4.5G_z + 1.065, \quad 0.01 \leq G_z \leq 0.03$$
$$A = 2.5G_z + 1.125, \quad 0.03 \leq G_z$$

While the aqueous resistance estimated by this method has been used extensively in calculating member permeability, several issues have not yet been resolved. First, in the MBLS scheme, the aqueous resistance is found to be independent of the membrane parameters, while Elliott's solution indicates that there is such a dependence. The significance of this dependence needs to be established. Second, the aqueous resistance of Eq. (6) has not been rigorously defined. Third, the accuracy of the MBLS has not been verified. To address these issues, a convective diffusive tube flow model was set up to analyze the concentration distribution within the tube interior. From these results, the aqueous resistance was quantitated and analyzed.

THEORY

The experimentally measured P_{eff} is an averaged quantity over the entire length of the tube as evidenced in Eq. (2). Consequently, it follows that the P_{aq} will necessarily be an averaged value as well. The purpose of the following derivation is to define this averaged quantity unambiguously. At steady state, the flux $J(z)$ through the intestinal membrane and aqueous boundary layer are equal, i.e.,

$$J(z) = P_{aq}(z)[C_c(z) - C_w(z)] = P_w(z)C_w(z) \tag{7}$$

where sink conditions are assummed on the serosal side of the intestinal membrane. Rigorously, J, P_{aq}, and P_w are z dependent. C_c and C_w are the concentrations at the center axis and tube wall, respectively. Since a spatially averaged quantity is sought, a mean $\overline{P_{aq}}$ can be defined by equating the integral membrane flux to the flux through a reference mean concentration gradient in the aqueous phase, i.e.,

$$\int_A P_w C_w dA = A\overline{P_{aq}}(\overline{C_c} - \overline{C_w}) \tag{8}$$

where the integral is evaluated over the intestinal membrane surface A. More generally, P_w is considered to be a combination of passive diffusion and carrier-mediated mechanisms in parallel as indicated in Eq. (3). Substituting Eq. (3) into Eq. (8) and setting $A = 2\pi RL$, the following expression for $\overline{P_{aq}}$ is obtained:

$$\overline{P_{aq}} = \frac{\int_0^L \left(\frac{J_{max}C_w}{K_m + C_w} + P_m C_w\right) dz}{[L(\overline{C_c} - \overline{C_w})]} \tag{9}$$

The quantities $\overline{C_c}$ and $\overline{C_w}$, yet to be defined, are the reference concentrations at the center axis and intestinal wall, respectively. They are simply taken to be the averages of their respective axially dependent quantities, i.e.,

$$\overline{C_c} = \frac{\int_0^L C_w \, dz}{L} \tag{10}$$

$$\overline{C_w} = \frac{\int_0^L C_c \, dz}{L} \tag{11}$$

It is apparent that, in order to evaluate $\overline{P_{aq}}$, one needs to know the concentrations at the wall and center axis. These quantities can be obtained by solving a mass transfer model with proper hydrodynamics incorporated.

The equation of continuity at steady state with axial convection and radial diffusion in cylindrical coordinates can be written as

$$V_z \frac{\partial C}{\partial z} = \frac{D}{r}\frac{\partial}{\partial r}\left(r\frac{\partial C}{\partial r}\right) \quad (12)$$

where V_z is the axial velocity profile. Since the model is not intended for analyzing the water transport, the radial convection term is not included in Eq. (12). It has been shown previously that laminar flow is the most appropriate model to be used for the perfusion system (10), hence the following expression is used:

$$V_z = V_{max}\left[1 - \left(\frac{r}{R}\right)^2\right] \quad (13)$$

Since the axial diffusion term was shown to be unimportant when compared to the convection term (8), it is not included in Eq. (12). The boundary conditions for the single-pass perfusion experiment are

$$\frac{\partial C}{\partial r} = 0, \qquad r = 0, \quad 0 \leq z \leq L \quad (14)$$

$$-D\frac{\partial C}{\partial r} = \frac{J_{max}C}{K_m + C} + P_m C, \qquad r = R, \quad 0 \leq z \leq L \quad (15)$$

$$C = C_o, \qquad z = 0, \quad 0 \leq r \leq R \quad (16)$$

The system can be simplified by dedimensionalization by substituting $\theta = C/C_o$, $\hat{z} = z/L$, and $\hat{r} = r/R$ into Eq. (12). The transformed equation then becomes

$$\frac{1 - \hat{r}^2}{G_z}\frac{\partial \theta}{\partial \hat{z}} = \frac{1}{\hat{r}}\frac{\partial \theta}{\partial \hat{r}} + \frac{\partial^2 \theta}{\partial \hat{r}^2} \quad (17)$$

with the boundary conditions,

$$\frac{\partial \theta}{\partial \hat{r}} = 0, \qquad \hat{r} = 0, \quad 0 \leq \hat{z} \leq 1 \quad (18)$$

$$\frac{\partial \theta}{\partial \hat{r}} = -\left(\frac{J^*_{max}/C_o}{K_m/C_o + \theta} + P^*_m\right)\theta, \qquad \hat{r} = 1, \quad 0 \leq \hat{z} \leq 1 \quad (19)$$

$$\theta = 1, \qquad \hat{z} = 0, \quad 0 \leq \hat{r} \leq 1 \quad (20)$$

The Graetz number, G_z, defined as $\pi DL/2Q$, is a dimensionless number which incorporates system dimensions and hydrodynamics. It is interpreted as the ratio of the mean axial residence time, $\pi R^2 L/Q$, to the mean radial diffusion time, $2R^2/D$. Therefore, G_z determines the importance of axial convection relative to radial diffusion. J^*_{max} and P^*_m are the normalized quantities obtained by multiplying J_{max} and P_m by R/D, respectively. The solution of the problem is clearly a function of spatial variables as well as G_z, J_{max}, K_m, P_m, and C_o. As such, it implies that $\overline{P_{aq}}$, as defined in Eq. (9), should also be a function of G_z and the membrane parameters.

RESULTS AND DISCUSSION

Numerical Accuracy

The nonlinearity in the boundary conditions precludes an analytical solution. The problem was then solved via a numerical finite-difference method. Discretization following the Crank Nicholson scheme results in a system of nonlinear algebraic equations which are solved by standard routines in the IMSL Mathematics Library. The solution obtained is the steady-state concentration profile in the intestinal lumen. The accuracy of the numerical solution was checked against Elliott's analytical solution to the first-order boundary condition case, i.e., with passive absorption at the wall (8). Table I is a comparison of the steady-state cup-mixing concentration, C_m/C_o, defined as

$$\frac{C_m}{C_o} = \frac{\int_0^{2\pi}\int_0^R V_z C r\, dr dz}{\int_0^{2\pi}\int_0^R V_z r\, dr dz} \quad (21)$$

at various G_z values. Since Elliott's solution is an infinite series, the values presented here are the approximation based on the first five terms. The numerical solution is calculated with a 20 × 20 grid mesh. Except at the high permeability and large G_z values, the numerical result is in excellent agreement with the exact solution, and the error is generally well below 1%.

Calculation of Mean Aqueous Resistance

Figure 1 illustrates a typical situation in a perfused intestine showing the axial dependence of $C_c/C_o(z)$, $C_w/C_o(z)$, and $1/P^*_{aq}(z)$ with $P^*_m = 1$ and $G_z = 0.05$. Here C_c/C_o and C_w/C_o are the dimensionless concentrations at the center axis and intestinal wall respectively; P^*_{aq} is the dimensionless aqueous permeability obtained by multiplying P_{aq} by R/D. Figure 1 shows that $C_w/C_o(z)$ decreases along the axial direction. Therefore, it is the concentration gradient, $C_c/C_o(z) - C_w/C_o(z)$, which is responsible for the aqueous resistance. With the concentration profile known from the numerical solution, one can evaluate the aqueous resistance, $P^{*-1}_{aq}(z)$, according to Eq. (7). It is shown in Fig. 1 that this resistance increases axially. If one defines the aqueous permeability, P_{aq}, as D/δ, where δ is the diffusion layer thickness, it is readily shown that the dimensionless aqueous resistance, $P^{*-1}_{aq}(z)$, is $\delta(z)/R$. Therefore, the aqueous resis-

Table I. Comparison of C_m/C_o Calculated from the Exact and Numerical Solutions to Eqs. (12)–(13) with Passive Absorption at the Wall, i.e., Eqs. (14–16) Assuming $J_{max} = 0$

G_z	Exact[a]	Numerical	% Error[b]
	$P^*_m = 0.01$		
0.001	0.9999	1.0000	(−0.01)
0.005	0.9988	0.9998	(−0.10)
0.01	0.9986	0.9996	(−0.10)
0.05	0.9970	0.9980	(−0.10)
0.1	0.9951	0.9961	(−0.11)
0.2	0.9911	0.9922	(−0.11)
	$P^*_m = 10$		
0.001	0.9763	0.9801	(−0.39)
0.005	0.9283	0.9300	(−0.18)
0.01	0.8808	0.8831	(−0.26)
0.05	0.6441	0.6501	(−0.93)
0.1	0.4626	0.4705	(−1.71)
0.2	0.2448	0.2531	(−3.39)

[a] See Ref. 8.

[b] Defined as [(exact − numerical)/exact] × 100%.

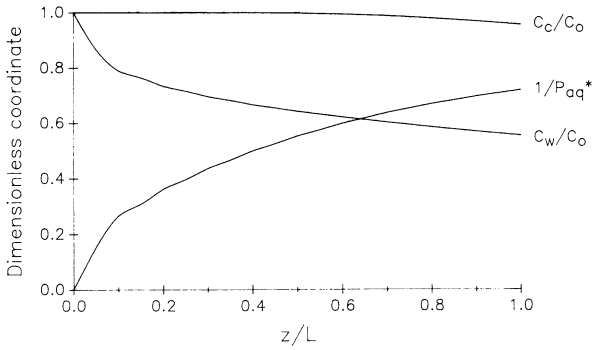

Fig. 1. A typical concentration and aqueous resistance profile in a perfused intestine: C_c/C_o, C_w/C_o, and $1/P^*_{aq}$ are dimensionless concentration at the center of the intestine, dimensionless concentration at the intestinal wall, and aqueous resistance in the lumen, respectively ($P^*_m = 1$ and $G_z = 0.05$).

tance plotted in Fig. 1 is actually the fractional diffusion layer thickness. The plot shows that this diffusion layer penetrates deep into the center of the tube under the flow and absorptive condition. In applying Eq. (1), it is understood that the aqueous resistance term is an spatially averaged quantity. As mentioned, it has not been made clear in the literature as to how this average quantity is obtained. The definition in Eq. (9) provides the missing link. As defined, $\overline{P_{aq}}$ is the mean value that gives the correct overall steady-state absorption rate. Figure 2 is the $\overline{P^*_{aq}}^{-1}$ plotted against G_z for passive absorption at the wall with $P^*_m = 0.1$, 1, and 10. Plotted in the graph also is the $\overline{P^*_{aq}}^{-1}$ calculated from the MBLS, i.e., Eq. (6). The numerical result demonstrates that the $\overline{P^*_{aq}}^{-1}$ is a function of not only G_z but also P^*_m. This is consistent with Elliott's solution, where C_m/C_o is dependent on P^*_m. In case of carrier-mediated mechanism at the wall, the dependence should also be extended to include J^*_{max}, K_m, and C_o. Figure 3 is the $\overline{P^*_{aq}}^{-1}$ versus G_z plot showing the P^*_c and K_m/C_o dependence. Here K_m/C_o indicates the relative saturation of the carrier binding sites and P^*_c is the carrier permeability, defined as J^*_{max}/K_m, which is essentially the dimensionless first-order permeability when $C_o << K_m$. These curves are obtained by solving Eqs. (17)–(20) in the absence of a passive mechanism, i.e., $P^*_m = 0$. The dependence of $\overline{P^*_{aq}}^{-1}$ on K_m/C_o is apparently rather weak. It

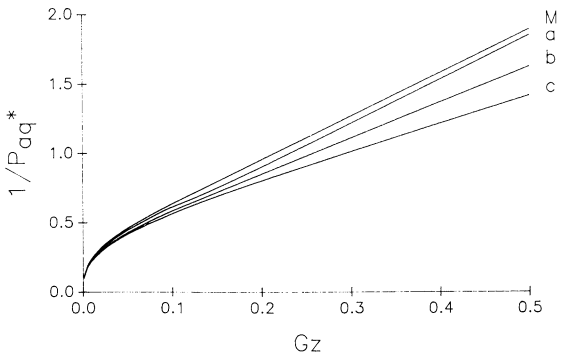

Fig. 2. A comparison of the mean aqueous resistance as a function of G_z calculated from the modified boundary layer solution (curve M) and the numerical solution with a P^*_m value of 10 (curve a), 1 (curve b), and 0.1 (curve c), respectively.

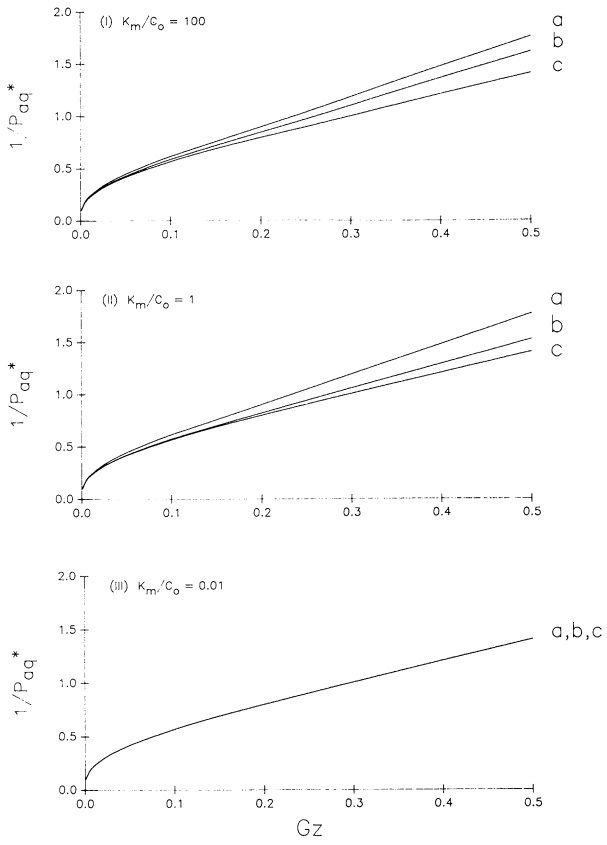

Fig. 3. A comparison of the mean aqueous resistance as a function of G_z calculated at K_m/C_o values of 100 (graph I), 1 (graph II), and 0.01 (graph III). Curves a, b, and c represent P^*_c values of 10, 1, and 0.1, respectively.

should also be noted that curves Ia, Ib, and Ic (Fig. 3) are the same as curves a, b, and c (Fig. 2), respectively. This is expected because in both cases the first-order absorption kinetics are operative at the wall. If C_o is increased such that $K_m/C_o = 0.01$, i.e., in the zero-order region, $\overline{P^*_{aq}}^{-1}$ for all three values of P^*_c, 0.1, 1, and 10, collapses into one curve as shown in Fig. 3, III. The results thus demonstrate that the aqueous resistance is clearly a function of G_z, J^*_{max}, K_m/C_o, and P^*_m in the most general case. The dependence grows as G_z is increased.

Accuracy of the Modified Boundary Layer Solution

In comparing the numerically calculated $\overline{P^*_{aq}}^{-1}$ with those calculated from MBLS, Fig. 2 shows that the latter is an approximation to the values calculated from the exact model, i.e., Eqs. (17)–(20). Over the range of G_z of practical interest, some differences are observed in $\overline{P^*_{aq}}^{-1}$. As a result of this difference, the error in P^*_w can be estimated as follows: the aqueous resistance $\overline{P^*_{aq,\epsilon}}^{-1}$ with error ϵ_{aq} can be defined by,

$$\frac{1}{\overline{P^*_{aq,\epsilon}}} = (1 + \epsilon_{aq})\frac{1}{\overline{P^*_{aq}}} \tag{22}$$

and the $P^*_{w,\epsilon}$ determined from Eq. (1) will be

$$P^*_{w,\epsilon} = \frac{\overline{P^*_{aq,\epsilon}} - P^*_{eff}}{P^*_{eff}\overline{P^*_{aq,\epsilon}}} \tag{23}$$

It can be shown that the error, ϵ_w, in the estimated $P^*_{w,\epsilon}$ is

$$\epsilon_w = \frac{P^*_w - P^*_{w,\epsilon}}{P^*_w} = \frac{-\epsilon_{aq}}{\Omega - \epsilon_{aq}} \tag{24}$$

where Ω is the ratio of wall resistance and aqueous resistance, $P^{*-1}_w/\overline{P^*_{aq}}^{-1}$. As an example, ϵ_{aq} at $G_z = 0.1$ are 0.122, 0.088, and 0.019 for P^*_m values of 0.1, 1, and 10, respectively; the resulting ϵ_w, in respective order, are -0.0070, -0.054, and -0.13. Since ϵ_w is dependent on Ω and ϵ_{aq}, as shown in Eq. (24), this error can be effectively controlled by making G_z small. The net effect is to make the Ω large while reducing ϵ_{aq}. If G_z is reduced to 0.01, ϵ_w become -0.0016, -0.014, and -0.056 for P^*_m values of 0.1, 1, and 10, respectively. Therefore, by careful control of the hydrodynamics, i.e., aqueous resistance, the MBLS solution can be used to obtain a good estimation of P^*_w.

Analysis of the Numerically Calculated Mean Aqueous Resistance

In order to use the numerically calculated aqueous resistance, it is advantageous to find a regressed function to represent the results. It was found that a function of the following form gives an excellent fit to the numerical values,

$$\overline{P^*_{aq}}^{-1} = AG_z^{1/3} + BG_z^C\left[P^*_c\left(\frac{K_m}{C_o}\right)^D + P^*_m\right]^E \tag{25}$$

where parameters A, B, C, D, and E are to be determined by regression analysis. The estimated parameters are summarized in Table II, with the range of applicability of

$$0.001 \leq G_z \leq 0.5$$
$$0.01 \leq P^*_m \leq 10$$
$$0.01 \leq P^*_c \leq 10$$
$$0.01 \leq K_m/C_o \leq 100.$$

The result indicates that the $\overline{P^*_{aq}}^{-1}$ has a weak dependence on the membrane parameters and a relatively strong dependence on the G_z value. Table III tabulated the numerical $\overline{P^*_{aq}}^{-1}$ values used in the regression and the percentage errors in the regressed value calculated by Eq. (25). Except in the large G_z range, the regressed function gives $\overline{P^*_{aq}}^{-1}$ values within 5% of the numerical values.

Table II. Parameters of Eq. (25) Estimated by Least-Squares Nonlinear Regression

Parameter	Estimated value[a]	SE	95% Confidence interval
A	1.05	0.0235	(1.00, 1.10)
B	1.74	0.0508	(1.64, 1.84)
C	1.27	0.0630	(1.14, 1.39)
D	0.0659	0.00482	(0.0563, 0.0754)
E	0.377	0.0556	(0.267, 0.487)

[a] The regression routine used is PCNONLIN, Statistical Consultants, Inc.

The functional form and the magnitude of the exponents of Eq. (25) suggest that there is a limiting behavior of G_z dependence. At small G_z, the second term in Eq. (25) drops out, leaving only a cube root dependence on G_z. Figure 4 is a plot of $\overline{P^*_{aq}}^{-1}$ versus $G_z^{1/3}$ showing this limiting behavior. Plotted also in Fig. 4 is the $\overline{P^*_{aq}}^{-1}$ calculated from Levich's solution. Essentially the Levich solution is a boundary layer solution to Eq. (12) with a sink condition at the wall (11). Using the definition in Eq. (9), the $\overline{P^*_{aq}}^{-1}$ calculated from Levich's solution is

$$\overline{P^*_{aq}}^{-1} = 0.995\, G_z^{1/3} \tag{26}$$

Details of the Levich model and derivation of $\overline{P^*_{aq}}^{-1}$ can be found in the Appendix. Figure 4 shows that the $\overline{P^*_{aq}}^{-1}$ calculated from the numerical results agrees excellently with those of Levich in the small G_z limit. This is the limit of entrance region where the thickness of the diffusion boundary layer is considerably smaller than the tube radius. Therefore, the linearization of the parabolic velocity profile is a good approximation. As the fluid moves further away from the entrance and into the tube, i.e., when G_z gets larger, the diffusional boundary layer grows farther into the lumen and the linearized velocity profile overestimates the convection effect. The extent of overestimation can be calculated by defining the error ϵ_v,

$$\epsilon_v = \frac{V_z' - V_z}{V_z} \tag{27}$$

where V_z is the parabolic velocity profile as defined in Eq. (13) and V_z' is the linearized profile used in Levich's model [see Eq. (A3)]. Putting Eqs. (13) and (A3) (see Appendix) into Eq. (27), the error ϵ_v is $(1 - \hat{r})^2/(1 - \hat{r}^2)$. Therefore, the errors are 5.26% at $\hat{r} = 0.9$, 33.3% at $\hat{r} = 0.5$, and at the worst case, 100% at $\hat{r} = 0$ (center axis). The effect of the overestimated axial convection is overestimating C_w, and this results in an underestimated $\overline{P^*_{aq}}^{-1}$, as evidenced in Fig. 4. The departure of curves a, b, and c (Fig. 4) from curve L indicates that the boundary layer assumption is no longer valid under these flow and absorptive conditions at the wall. Since the divergence occurs at a G_z value as low as 0.001 and a typical experimental G_z value can be as high as 0.1, the boundary layer approach may not give an accurate $\overline{P^*_{aq}}^{-1}$ estimation. As mentioned, the model developed in this work is most general, requiring no simplifying assumptions; therefore, the $\overline{P^*_{aq}}^{-1}$ derived from its solution will have a full range of validity.

In practice, the membrane permeability can be calculated from the experimental C_m/C_o and G_z values by an iterative method using Eqs. (1), (2), and (25). As an example, the dimensionless passive permeability of phenytoin is calculated from the experimental data as illustrated in Table IV (12). Without any prior knowledge of the permeability of phenytoin, an initial guess of $P^*_m = 100$ is used to estimate the $\overline{P^*_{aq}}^{-1}$ by Eq. (25). The $1/P^*_{eff}$ term is calculated from the experimental C_m/C_o and G_z values using the dimensionless form of Eq. (2), i.e., $1/P^*_{eff} = -4G_z[\ell n(C_m/C_o)]^{-1}$. The $1/P^*_w$ is then calculated by Eq. (1). This P^*_w is then used to make a new estimate of $\overline{P^*_{aq}}^{-1}$ and a new P^*_w can be calculated. The

Table III. Table of $\overline{P^*_{aq}}^{-1}$ Calculated Numerically from the Model and Errors in Regressed Values

G_z	$P^*_c = 0.01$	$P^*_c = 0.1$	$P^*_c = 1$	$P^*_c = 10$
		$K_m/C_o = 100$ and $P^*_m = 0$		
0.001	0.1027 (−2.71)[a]	0.1025 (−2.94)	0.1033 (−2.19)	0.1053 (−0.29)
0.005	0.1735 (−4.68)	0.1742 (−4.43)	0.1755 (−3.84)	0.1812 (−0.79)
0.01	0.2225 (−3.73)	0.2232 (−3.71)	0.2255 (−3.01)	0.2338 (−0.25)
0.025	0.3153 (−1.76)	0.316 (−2.24)	0.3208 (−1.51)	0.3341 (−1.64)
0.05	0.4174 (−0.53)	0.4189 (−1.43)	0.4278 (−0.76)	0.4467 (−1.89)
0.075	0.4968 (−0.11)	0.4991 (−1.42)	0.5122 (−0.84)	0.536 (−1.4)
0.1	0.5656 (−0.02)	0.5688 (−1.7)	0.5865 (−1.16)	0.615 (−0.71)
0.2	0.7973 (−0.59)	0.8054 (−3.4)	0.8468 (−2.57)	0.8983 (−1.32)
0.5	1.4095 (−1.67)	1.4371 (−6.55)	1.6168 (−1.78)	1.7616 (−0.97)
		$K_m/C_o = 1$ and $P^*_m = 0$		
0.001	0.1029 (−2.48)	0.1029 (−2.51)	0.103 (−2.45)	0.1042 (−1.32)
0.005	0.174 (−4.28)	0.1741 (−4.36)	0.1745 (−4.29)	0.179 (−1.86)
0.01	0.2229 (−3.34)	0.223 (−3.56)	0.2237 (−3.56)	0.2314 (−0.47)
0.025	0.3154 (−1.27)	0.3156 (−1.83)	0.3172 (−2.04)	0.332 (−1.71)
0.05	0.4177 (−0.38)	0.418 (−0.68)	0.4213 (−1.19)	0.4456 (−2.89)
0.075	0.4972 (−1.15)	0.4977 (−0.34)	0.503 (−1.11)	0.5357 (−3.06)
0.1	0.5662 (−1.58)	0.5668 (−0.33)	0.5744 (−1.31)	0.6155 (−2.95)
0.2	0.7989 (−2.15)	0.8005 (−1.08)	0.8207 (−2.48)	0.9013 (−2.56)
0.5	1.407 (−2.75)	1.415 (−2.89)	1.527 (−2.02)	1.774 (−5.5)
		$K_m/C_o = 0.01$ and $P^*_m = 0$		
0.001	0.1029 (−2.46)	0.1029 (−2.49)	0.1029 (−2.52)	0.1029 (−2.56)
0.005	0.174 (−4.18)	0.174 (−4.31)	0.174 (−4.46)	0.174 (−4.64)
0.01	0.2229 (−3.15)	0.2229 (−3.4)	0.2229 (−3.69)	0.2229 (−4.02)
0.025	0.3154 (−0.86)	0.3154 (−1.42)	0.3154 (−2.06)	0.3154 (−2.82)
0.05	0.4176 (−1.11)	0.4176 (−0.1)	0.4176 (−1.08)	0.4176 (−2.45)
0.075	0.4972 (−2.2)	0.4972 (−0.78)	0.4972 (−0.87)	0.4972 (−2.79)
0.1	0.5661 (−2.89)	0.5661 (−1.09)	0.5661 (−0.99)	0.5661 (−3.42)
0.2	0.7987 (−4.39)	0.7987 (−1.33)	0.7987 (−2.24)	0.7987 (−6.38)
0.5	1.4063 (−6.82)	1.4063 (−1.26)	1.4063 (−5.21)	1.4067 (−12.7)
G_z	$P^*_m = 0.01$	$P^*_m = 0.1$	$P^*_m = 1$	$P^*_m = 10$
		$P^*_c = 0$		
0.001	0.1029 (−2.48)	0.1029 (−2.51)	0.1033 (−2.16)	0.1053 (−0.26)
0.005	0.174 (−4.28)	0.1742 (−4.3)	0.1755 (−3.7)	0.1812 (−0.63)
0.01	0.223 (−3.29)	0.2232 (−3.47)	0.2255 (−2.73)	0.2338 (−0.56)
0.025	0.3154 (−1.27)	0.316 (−1.7)	0.3209 (−0.86)	0.3341 (−2.33)
0.05	0.4178 (−0.41)	0.4189 (−0.46)	0.4279 (−0.37)	0.4467 (−3.13)
0.075	0.4974 (−1.19)	0.4991 (−0.06)	0.5124 (−0.75)	0.536 (−3.12)
0.1	0.5664 (−1.61)	0.5688 (−0.03)	0.5867 (−0.82)	0.615 (−2.87)
0.2	0.7994 (−2.21)	0.8054 (−0.47)	0.8471 (−0.71)	0.8983 (−2.24)
0.5	1.4095 (−2.93)	1.438 (−1.24)	1.618 (−3.72)	1.8433 (−9.05)

[a] Numbers in parentheses are percentage errors in regressed values, calculated by Eq. 25, relative to numerical values.

iteration continues until P^*_w converges. As shown in Table IV, the convergence is rather fast regardless of the initial estimate of $P^*_{m,g}$. This iteration method can also be applied to the case of Michaelis Menton absorption at the wall.

CONCLUSIONS

In summary, the aqueous resistance in a perfused tube was unambiguously defined and calculated at various flow and absorptive conditions. The calculation is based on the numerical solution to the exact convective diffusive mass transport problem without any simplifying assumptions. The results demonstrate that the $\overline{P^*_{aq}}^{-1}$ is a function of G_z as well as membrane parameters, namely, P^*_m, J^*_{max}, and K_m/C_o. These numerically calculated aqueous resistances at various G_z and permeability values was fitted to a functional equation [Eq. (25)], and the result indicates that the dependence on permeability and Michaelis constant is relatively weak

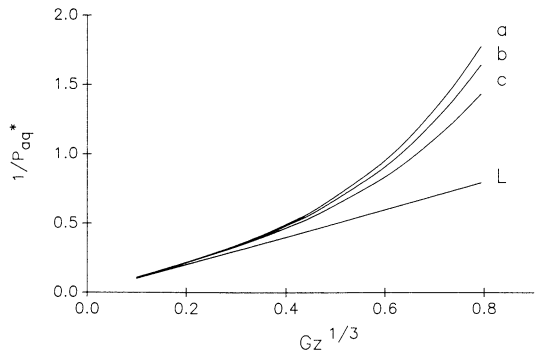

Fig. 4. A comparison of $\overline{P^*_{aq}}^{-1}$ calculated from the numerical (curves a, b, and c) and Levich (curve L) solutions. Curves a, b, and c are reproduced from Fig. 3, I.

when compared to G_z. This equation is found to converge to the Levich limit only in the low-G_z value region, thus indicating the limitation of the boundary layer approach. Since Eq. (25) is derived from an exact model, it should have a full range of validity. The practical utility of Eq. (25) in extracting true membrane permeability was also demonstrated by the phenytoin example.

APPENDIX

Derivation of $\overline{P^*_{aq}}^{-1}$ from Levich's Solution to a Convective Diffusive Tube Flow Problem

Levich's problem concerns flow in the interior of a tube in which the tube wall acts as a sink to the solute of interest (11). The steady-state concentration of the solute is governed by

$$V_z \frac{\partial C}{\partial z} = \frac{D}{r}\frac{\partial}{\partial r}\left(r\frac{\partial C}{\partial r}\right) \tag{A1}$$

where V_z is a laminar velocity profile,

$$V_z = V_{max}\left[1 - \left(\frac{r}{R}\right)^2\right] \tag{A2}$$

Table IV. An Iteration Scheme Using Eqs. (1), (2), and (25) to Calculate the True Membrane Permeability of Phenytoin from Experimental Data (12)

Iteration	G_z	C_m/C_o	$1/P^{*\,a}_{eff}$	$P^{*\,b}_{m,g}$	$1/\overline{P^{*\,c}_{aq}}$	$P^{*\,d}_{w}$
1	0.0410	0.760	0.598	100	0.533	15.5
2	0.0410	0.760	0.598	15.5	0.447	6.63
3	0.0410	0.760	0.598	6.63	0.424	5.75
4	0.0410	0.760	0.598	5.75	0.420	5.64
5	0.0410	0.760	0.598	5.64	0.420	5.63
1	0.0410	0.760	0.598	0.001	0.364	4.29
2	0.0410	0.760	0.598	4.29	0.414	5.45
3	0.0410	0.760	0.598	5.45	0.419	5.61
4	0.0410	0.760	0.598	5.61	0.420	5.62
5	0.0410	0.760	0.598	5.62	0.420	5.63

[a] Calculated by $[-4G_z/\ln(C_m/C_o)]$.
[b] $P^*_{m,g} \rightarrow P^*_w$ except that the first value is an initial guess.
[c] Calculated by Eq. (25) with $P^*_c = 0$, and $P^*_m = P^*_{m,g}$.
[d] Calculated by Eq. (1).

Taking a boundary layer approach assuming diffusion occurs only over a small distance from the wall, the problem is transformed onto semiinfinite coordinates with a new radial variable y defined as $R - r$. For small y, the laminar profile can be approximated by,

$$V_z = V_{max}\left(\frac{2y}{R}\right) \tag{A3}$$

and the PDE becomes

$$\frac{2V_{max}y}{R}\frac{\partial c}{\partial z} = D\frac{\partial^2 c}{\partial y^2} \tag{A4}$$

with the boundary conditions

$$C = C_o, \quad y \rightarrow \infty, \quad 0 \leq z \leq L \tag{A5}$$

$$C = 0, \quad y = 0, \quad 0 \leq z \leq L \tag{A6}$$

$$C = C_o, \quad z = 0, \quad 0 \leq y \tag{A7}$$

Equation (A4) is solved by introducing a new variable η,

$$\eta = \left(\frac{V_{max}}{DR}\right)^{1/3} y\, x^{-1/3} \tag{A8}$$

Upon solving the system, the diffusional flux, J, through the wall is given by

$$J = D\left(\frac{\partial c}{\partial y}\right)_{y=0} = 0.67C_oD\left(\frac{V_{max}}{DR_z}\right)^{1/3} \tag{A9}$$

Using Eq. (8), the $\overline{P_{aq}}$ is determined by

$$\overline{P_{aq}} = \frac{\int_A JdA}{A(\overline{C_c} - \overline{C_w})} \tag{A10}$$

Putting $\overline{C_c} = C_o$, $\overline{C_w} = 0$, $A = 2\pi RL$ and substituting Eq. (A9) into (A10), the result is $\overline{P_{aq}} = 1.005\,(D/R)G_z^{-1/3}$, which gives the mean aqueous resistance,

$$\overline{P^*_{aq}}^{-1} = 0.995G_z^{1/3} \tag{A11}$$

ACKNOWLEDGMENTS

This work was supported by NIH Grants 1R29NS24616-03 and GM37188. Jim Kou would like to acknowledge the assistance in nonlinear regression work by Dr. Doron I. Friedman.

REFERENCES

1. D. Winne. Dependence of Intestinal absorption in vivo on the unstirred layer. *Naunyn-Schmiedeberg Arch. Pharmacol.* **304**: 175–181 (1978).
2. I. Komiya, J. Y. Park, A. Kamani, N. F. H. Ho, and W. I. Higuchi. Quantitative mechanistic studies in simultaneous fluid flow and intestinal absorption using steroids as model solutes. *Int. J. Pharm.* 4:249–262 (1980).
3. A. B. R. Thomson and J. M. Diestchy. Derivation of the equations that describe the effects of unstirred water layers on the kinetic parameters of active transport processes in the intestine. *J. Theor. Biol.* 64:277–294 (1977).

4. H. Yuasa, Y. Miyamoto, T. Iga, and M. Hanano. Intestinal absorption by carrier-mediated transports: Two dimensional laminar flow model. *J. Theor. Biol.* **119**:25–36 (1986).
5. D. Winne. Unstirred layer, source of biased Michaelis constant in membrane transport. *Biochim. Biophys. Acta* **298**:27–31 (1973).
6. D. Winne. Correction of the apparent Michaelis constant, biased by an unstirred layer, if a passive transport component is present. *Biochim. Biophys. Acta* **464**:118–126 (1977).
7. N. F. H. Ho and W. I. Higuchi. Theoretical model studies of intestinal drug absorption. IV. Bile acid transport at premicellar concentrations across diffusion layer-membrane barrier. *J. Pharm. Sci.* **63**:686–690 (1974).
8. R. L. Elliott, G. L. Amidon, and E. N. Lightfoot. A convective mass transfer model for determining intestinal wall permeabilities: Laminar flow in a circular tube. *J. Theor. Biol.* **87**:757–771 (1980).
9. D. A. Johnson and G. L. Amidon. Determination of intrinsic membrane transport parameters from perfused intestine experiments: A boundary layer approach to estimating the aqueous and unbiased membrane permeabilities. *J. Theor. Biol.* **131**:93–106 (1988).
10. G. L. Amidon, J. Kou, R. L. Elliott, and E. N. Lightfoot. Analysis of models for determining intestinal wall permeabilities. *J. Pharm. Sci.* **69**:1369–1373 (1980).
11. V. G. Levich. In *Physicochemical Hydrodynamics,* Prentice Hall, Englewood Cliffs, N.J., 1962, p. 112.
12. D. Fleisher. Unpublished result (1988).